Received: 23 June 2025 | Accepted: 9 April 2026

DOI: 10.1002/saj2.70254

Soil Science Society of America Journal

ORIGINAL ARTICLE

Soil and Ecosystem Processes

Mineral-associated organic matter and soil health indicators in subsiding cultivated histosols of the Everglades Agricultural Area

Mumtahina Riza[1] | **Suraj Melkani**[2,3] | **Noel Manirakiza**[2,3] | **Jehangir H. Bhadha**[2,3] | **Zihan Li**[4] | **Jing Hu**[4] | **Lisa G. Chambers**[1]

[1]Aquatic Biogeochemistry Laboratory, Department of Biology, University of Central Florida, Orlando, Florida, USA

[2]Soil, Water and Ecosystem Sciences Department, Institute of Food and Agricultural Sciences, University of Florida, Gainesville, Florida, USA

[3]Everglades Research and Education Center, Institute of Food and Agricultural Sciences, University of Florida, Belle Glade, Florida, USA

[4]Department of Civil, Environmental, and Construction Engineering, University of Central Florida, Orlando, Florida, USA

Correspondence
Lisa G. Chambers, Department of Biology, University of Central Florida, 4000 Central FL Blvd., Bldg 20, BIO 301, Orlando, FL 32816, USA. Email: lisa.chambers@ucf.edu

Assigned to Associate Editor Rongzhong Ye.

Funding information
National Institute of Food and Agriculture, Grant/Award Number: 2023-67019-39834; U.S. Department of Agriculture; University of Central Florida

Abstract

Soil drainage leads to subsidence in organic-rich peat soils (histosols) due to compaction and accelerated soil oxidation, removing carbon (C). Research suggests mineral-associated organic matter (MAOM) promotes soil C persistence, but the prevalence of MAOM in cultivated histosols and its relationship with commonly measured soil health indicators (SHIs) are unknown. The objectives of this study were to (1) quantify soil C fractions and diverse SHIs in the Everglades Agricultural Area, Florida, to comprehensively evaluate the soil condition, and (2) determine if any existing SHIs, general soil properties, depth, or profile thickness may predict MAOM abundance. Soil cores were collected at 15 locations and up to 45-cm depth. Profile thickness (a proxy for oxidation) was determined by probing to bedrock, and C fractionation included both physical and density separation. Soil organic matter (SOM) content averaged 62% by mass, with nearly 50% of the soil aggregates >2 mm. Potassium-permanganate oxidizable C averaged 28.2 ± 0.9 g kg^{-1}, and organic C concentration was five times greater than inorganic C. Particulate organic matter-Carbon (POM-C) accounted for >99% of soil (220.6 ± 9.3 g kg^{-1}), while mineral-associated organic matter-Carbon (MAOM-C) represented <1% (0.3 ± 0.1 g kg^{-1}). POM-C was predicted by soil profile thickness and several SHIs, but MAOM-C was not well predicted by almost any parameter measured. Results emphasize the predominance of unassociated organic C and suggest MAOM may serve as a unique SHI for organic soils. Management practices should focus on preventing further loss of vulnerable POM-C and promoting MAOM-C formation.

Abbreviations: ASI, aggregate stability index; CEC, cation exchange capacity; EAA, Everglades Agricultural Area; IC, inorganic carbon; LOI, loss-on-ignition; MAOM, mineral-associated organic matter; MAOM-C, Carbon within the mineral-associated organic matter; OC, organic carbon; PLS-SEM, partial least squares structural equation modeling; POM, particulate organic matter; POM-C, Carbon within the particulate organic matter; POXC, permanganate oxidizable carbon; SHI, soil health indicator; SOC, soil organic carbon; SOM, soil organic matter; TC, total carbon; TK, total potassium; TKN, total Kjeldahl nitrogen; TN, total nitrogen; TP, total phosphorus.

Plain Language Summary

Draining organic-rich peat soil causes subsidence over time and soil carbon is lost. Scientists believe that carbon bound to minerals, called mineral-associated organic matter (MAOM), lasts longer in soils, but little is known about how much MAOM exists in cultivated peat soils or whether common soil health tests can detect it. In this study, we examined soils from the Everglades Agricultural Area in Florida to measure different forms of soil carbon and a wide range of soil health indicators. Soil cores were collected from 15 locations down to 45 cm, and soil thickness was used as a proxy of past soil oxidation. More than 99% of soil carbon was particulate organic matter (loose, plant-derived material), while less than 1% was MAOM-C (stable soil carbon pool). Common soil health indicators could explain changes in particulate carbon, but they did not reliably predict MAOM. Protecting soil from further carbon loss and finding ways to increase MAOM may help slow peat soil degradation.

1 | INTRODUCTION

Soil organic carbon (SOC) is the largest constituent (50%–58%) of soil organic matter (SOM) and plays a critical role in carbon (C) sequestration and global climate regulation (Conchedda & Tubiello, 2020; Nelson & Sommers, 1996; Tiemeyer et al., 2020). Many climate-smart agricultural management strategies aim to enhance SOC storage to improve soil fertility and mitigate climate change (Lessmann et al., 2022). Understanding the mechanisms that promote SOC persistence and reduce its vulnerability to mineralization is therefore key for sustaining soil health. The stabilization of SOM occurs through several mechanisms, including (1) physical protection within aggregates, (2) physicochemical interactions with mineral surfaces and metal ions, and (3) biochemical resistance of complex organic compounds (Rowley et al., 2018; Six et al., 2002; Von Lützow et al., 2007). Among these mechanisms, physicochemical stabilization through mineral associations has received increasing attention because SOM bound to mineral surfaces exhibits longer turnover times than unassociated particulate organic matter (POM) or aggregates (Feng et al., 2013; Jagadamma et al., 2014). This stabilization pathway forms mineral-associated organic matter (MAOM), defined as organic compounds that are sorbed to fine mineral particles such as silt and clay. Recent advances in soil C research emphasize the conceptual framework separating SOM into POM and MAOM pools, which differ in formation pathways, persistence, and sensitivity to environmental and management factors (Cotrufo et al., 2019; Lavallee et al., 2020). Particulate organic matter reflects recent plant residues with rapid turnover, whereas MAOM is formed primarily through microbial processing of organic substrates followed by sorption onto mineral surfaces, resulting in a more persistent SOC pool (Cotrufo et al., 2019). Since MAOM is less susceptible to decomposition, it is a critical component of long-term soil C storage and soil resilience.

Despite a growing focus on MAOM within soil C research, common soil health indicator (SHI) frameworks do not explicitly quantify mineral-associated C pools. Existing frameworks, such as the Soil Management Assessment Framework (Andrews et al., 2004; Wienhold et al., 2009), the comprehensive assessment of soil health (Moebius-Clune, 2016), and the Soil Health Institute framework (Bagnall et al., 2023), evaluate a range of biological, chemical, and physical indicators but not MAOM, an indicator of C stabilization. Consequently, MAOM is rarely measured alongside other SHIs. We posit that quantifying MAOM with established SHIs will provide a more comprehensive assessment of soil C stability and soil health, which is critically important in subsiding or degraded soils.

The Everglades Agricultural Area (EAA) in south-central Florida provides an ideal case study for assessing C stability and SHIs in tandem with cultivated histosols. Over the past century, drainage-induced oxidation has resulted in approximately 2 m of soil surface elevation loss and 4.9×10^8 Mt of CO_2 flux emissions from the region (Aich et al., 2013). Average subsidence (2010–2019) was 0.63 cm year^{-1} (J. H. Bhadha et al., 2020) with a projected elevation drop of an additional 36 cm by 2068 (Rodriguez et al., 2020). In some locations, underlying limestone bedrock is exposed, highlighting the vulnerability of remaining soil and the need to enhance C stability for long-term agricultural productivity (Bai et al., 2024). Previous soil health research in the EAA has largely focused on nutrient cycling, microbial activity, and environmental conditions that influence SOM decomposition (e.g., redox dynamics, enzyme activity, and nutrient availability) (J. Bhadha et al., 2018; Osborne et al., 2017; Wright & Inglett, 2009). While prior studies have improved the understanding of the biological and chemical functioning of EAA soils,

most have evaluated soil C as one total pool, rather than fractionating SOM by stability, and no prior work in the EAA has quantified MAOM-carbon (C). This has created a key knowledge gap regarding the form and persistence of SOM in EAA soils. It is predicted that progressive subsidence that increases histosol-bedrock interactions in the EAA may provide reactive mineral surfaces for MAOM-C formation, but the availability of clay-sized particles for organic matter binding (Kögel-Knabner et al., 2008) is largely unknown in this system.

The objectives of this study were to (1) quantify MAOM and existing SHIs across multiple locations in the EAA by soil sampling depth (0–15, 15–30, and 30–45 cm) and soil profile thickness levels (shallow [0–60 cm], middle [0–90 cm], and deep [0–150 cm]), and (2) determine whether soil C stability fractions (MAOM-C and POM-C) can be predicted by SHIs, soil properties, sampling depth, or soil profile thickness as a proxy for the degree of soil oxidation. An improved understanding of MAOM-C abundance and its relationships to other soil properties and SHIs will inform management strategies to slow oxidation and sustain agricultural productivity in the EAA and similar cultivated histosols.

Core Ideas

- All soil health indicators (SHIs) were broadly uniform across sampling depths except biological properties, likely due to agricultural practices.
- Mineral-associated organic matter-Carbon (MAOM-C) exhibited no significant associations with sampling depth, soil profile thickness, or SHIs.
- Unassociated particulate organic matter-Carbon (POM-C) dominated the cultivated histosols and varied with sampling depth.
- MAOM may be applied as a practical SHI to assess soil stability in organic soil systems.

2 | MATERIALS AND METHODS

2.1 | Study site description

The entire EAA encompasses an area of 2872 km^2 south of Lake Okeechobee and north of Everglades National Park (Izuno et al., 1991). Soils at the study locations are classified as histosols (USDA Soil Taxonomy), primarily belonging to the Pahokee, Terra Ceia, Lauderhill, and Dania series and are classified as Euic, thermic to hyperthermic Typic Haplosaprists and Euic, hyperthermic Lithic Haplosaprists; these sapric peats are derived from decomposed sawgrass (*Cladium jamaicense*) (Soil Survey Staff, 2022). Seven soil series can be found in the EAA: Torry, Terra Ceia, Okeechobee, Pahokee, Lauderhill, Dania, and Okeelanta (Bottcher & Izuno, 1994; Rice et al., 2005). Among these soil types, Torry, Terra Ceia, and Okeechobee have the deepest thickness of organic material (>130 cm), Pahokee has the deeper O horizon (91–130 cm), followed by Lauderhill (51–91 cm) and Dania (<51 cm) (Rice et al., 2005). Oxidation caused by drainage has converted the high-fiber "sawgrass peats" of the early 1900s into low-fiber "mucks," reducing the percentage of Torry, Terra Ceia, and Okeechobee soils and creating shallower Pahokee and Lauderhill soil series (Rice et al., 2005). Presently, 85.4% of the farmland within the EAA is cultivated with sugarcane; the remaining agricultural land is rotated between winter vegetables and rice (J. Bhadha et al., 2018). The study site specifications are given in Table S1.

2.2 | Experimental design

The EAA was subdivided into four quadrants to ensure regional spatial coverage. An observational, stratified random sampling design was employed, with stratification based on total soil profile thickness as a proxy for long-term oxidation (i.e., utilizing the assumption that shallower profiles reflect greater oxidation and deeper profiles indicate lower oxidation). Soil profile thickness was recorded as a continuous measurement but treated as a categorical variable with three bins: shallow (0–60 cm), middle (0–90 cm), and deep (0–150 cm), which guided sampling location selection. Since samples from the three sampling depths (0–15, 15–30, and 30–45 cm) at each location originated from the same soil profile, observations were not independent within profiles. Five locations were randomly selected within each profile thickness bin, resulting in a total of 15 sampling locations. Soil profile thickness was determined by inserting a metal soil probe into the soil until it encountered resistance from the underlying bedrock. The depth of the probe was measured and recorded for three spots within an area of 1 m in diameter and averaged to determine the thickness of the soil profile. Land cover was not used for stratification because all locations were privately managed agricultural fields with rotating crops, making land-use classes inconsistent and nonrepresentative for stratified sampling. Moreover, the history of management practices was not available due to restrictions on the consent of the landowners.

2.3 | Field sample collection

Soil samples were collected from 15 locations in August and September 2023 (Figure 1). All locations were in agricultural fields cultivated with sugarcane, flooded rice, or fallow during

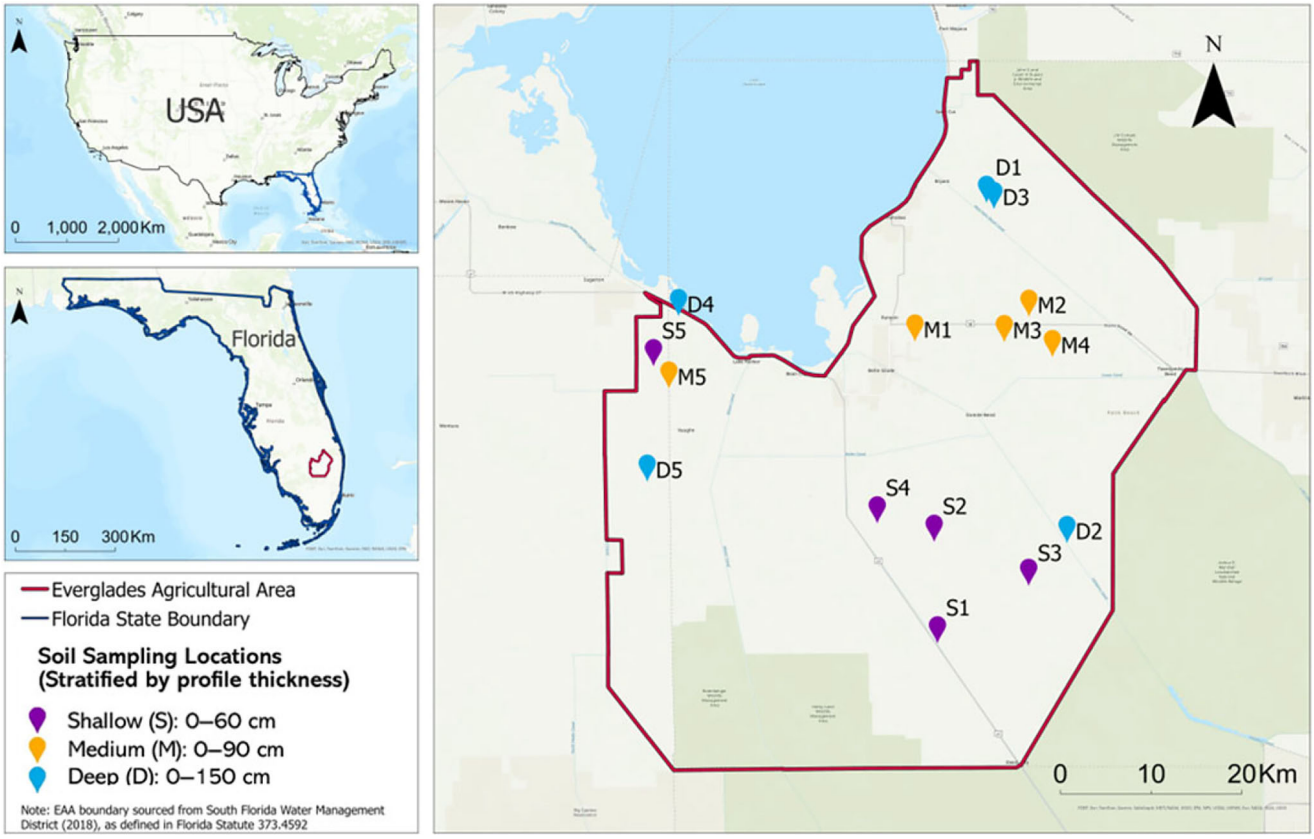

FIGURE 1 Sampling locations across the Everglades Agricultural Area (EAA) based on the total soil profile thickness: shallow (S1–S5), middle (M1–M5), and deep (D1–D5). Soil samples were collected at three depths (0–15, 15–30, and 30–45 cm) from each location.

sampling during late wet-season conditions. At each sampling location, triplicate soil samples (within 1 m) were collected from 0–15, 15–30, and 30–45 cm using an open-faced auger (6.7 cm inner diameter, 30 cm barrel) and composited. As the effective recoverable core length per extraction is 15 cm, sampling was conducted sequentially in 15-cm increments. Samples were placed in a labeled gallon-sized Ziplock™ bag and stored on ice. The 0-45 cm total sampling depth was selected to represent the zone of greatest C input, microbial activity, and management influence, making it sensitive for evaluating C stability and soil health. Within hours of collection, soils were divided into two subsamples and frozen at $-4 \pm 2^{\circ}C$ at the Everglades Research and Education Center (EREC) at the University of Florida. One subsample remained at EREC for biological and select chemical property analysis (i.e., enzyme assays, soil protein, cation exchange capacity [CEC], bulk density, total Kjeldahl nitrogen [TKN], and TK). The other subsample was transported in ice to the University of Central Florida Aquatic Biogeochemistry Laboratory for analysis of the remaining soil properties. At the time of sampling, a hand-held GPS device (Multiband RTK GNSS Receiver (RS 2+), Emlid) was used to record the coordinates of each location.

2.4 | Laboratory analysis

2.4.1 | Physicochemical properties

After thawing and homogenizing by hand, soil subsamples were oven-dried at 70°C to constant weight to determine moisture content. Tapped bulk density was estimated following the method described by Jacobs et al. (1964). Air-dried (<2 mm) soil was placed in a graduated cylinder and tapped under a standardized protocol until volume stabilized, and density was calculated as dry mass divided by settled volume. Since this method uses disturbed soil, the values represent tapped bulk density rather than true in situ bulk density.

Aggregate stability index (ASI) was determined using 50 g of field-moist soil placed on a stack of sieves (8 mm, 5.6 mm, 4 mm, 2 mm, 250 μm, and 53 μm) following the wet-sieving method of Karami et al. (2012). Field-moist soil was used to avoid artificial strengthening of aggregates caused by drying (Kaiser et al., 2015; Mirabito & Chambers, 2023). The sieve stack was placed in a Yoder-type wet sieve shaker (Yatherm Scientific) filled with tap water and shaken vertically (3–4 cm amplitude, 30 cycles min^{-1}) for 2 min (Kemper & Rosenau, 1986). Aggregates retained on each sieve were

collected, oven-dried at 70°C, and weighed to determine the proportion of each size fraction. Fractions were categorized as large macroaggregates (>2 mm), macroaggregates (250 µm–2 mm), and microaggregates (53–250 µm). The silt + clay fraction (<53 µm) was calculated as the difference between the initial sample mass and the sum of the retained fractions. Due to the nature of the analysis, ASI results were presented as a percentage of the total soil mass, rather than the C content of each fraction.

Mineral-associated organic matter (MAOM) was quantified by physical fractionation based on particle size following Six et al. (1998). Approximately 35 g of field-moist soil was placed in a 250-mL Nalgene bottle with 0.5% sodium hexametaphosphate at a 1:8 soil-to-solution ratio to disperse aggregates (Cambardella & Elliott, 1992; Mirabito & Chambers, 2023). The suspension was shaken at 150 rpm for 18 h and then wet-sieved through a 53-µm sieve by raising and resubmerging the sieve 50 times over 2 min (Cambardella & Elliott, 1993). The material retained on the sieve (>53 µm) was collected as POM, while the <53 µm fraction was considered as MAOM. Both fractions were oven-dried at 70°C to constant weight prior to further analysis. Next, a 3 g subsample of the <53 µm fraction was placed in a 50 mL centrifuge tube with 30 mL deionized (DI) water and centrifuged at 3500 rpm for 30 min to remove water-soluble C, after which the supernatant was filtered and discarded (Ghani et al., 2003). Subsequently, 20 mL of 1.85 g cm^{-3} sodium polytungstate (SPT) was added, and the sample was centrifuged at 5000 rpm for 30 min at 20°C to separate light fractions (LFs) and heavy fractions (HFs) (Mirabito & Chambers, 2023). The floating LF was filtered through a 0.45-µm nylon filter, rinsed with DI water to remove SPT, and collected. If separation was incomplete, centrifugation and filtration were repeated. The remaining HF was transferred with DI water to a pre-weighed container. Both fractions were oven-dried at 70°C to constant weight. The LF was considered free POM and combined with the >53 µm POM fraction from physical fractionation, while the <53 µm HF was considered MAOM (Six et al., 1998). Dried samples were ground using ceramic balls in a SPEX 8000 M Mixer/Mill (SPEX SamplePrep) and stored for subsequent determination of total C (TC) as MAOM-C and POM-C.

Soil pH was measured using a pH meter (Accumet, Fisher Scientific) in a 1:5 soil-to-water slurry. CEC was determined by the ammonium acetate method (Chapman, 1965; Nelson & Sommers, 1996), where soils were leached with 1 N ammonium acetate to displace exchangeable cations, washed with alcohol to remove excess ammonium, and exchangeable ammonium was quantified to calculate CEC. Soil protein was measured using the sodium citrate extraction method (Schindelbeck et al., 2016). Briefly, 1.5 g of soil was extracted with 12 mL of 0.02 M sodium citrate (pH 7), autoclaved at 121°C for 30 min, shaken for 30 min, and centrifuged. An aliquot (90 µL) of the extract was reacted with 1.8 mL bicinchoninic acid (BCA) reagent, incubated at 60°C for 30 min, and absorbance was measured at 562 nm to quantify protein concentration using the Thermo Pierce Colorimetric BCA.

Loss-on-ignition (LOI) method was applied to determine SOM. Oven-dried soil (~70°C) was ground using a SPEX SamplePrep 8000 M Mixer/Mill and combusted at 550°C in a muffle furnace to calculate SOM by mass loss. Particle size distribution of the mineral fraction (ash remaining after LOI) was measured using a CILAS 1190 laser particle size analyzer (Cilas) in wet mode. The <250 µm fraction was isolated by sieving, and approximately 0.5–1.0 g was dispersed in 4% sodium hexametaphosphate and shaken at 150 rpm for 24 h. An aliquot of the slurry was analyzed at 10%–20% obscuration, and clay (<2 µm), silt (2–50 µm), fine sand (50–250 µm), and coarse sand (>250 µm) fractions were determined as the average of two measurements.

TKN was determined by acid digestion followed by colorimetric analysis according to EPA Method 351.2. Approximately 0.2 g of soil was digested with 2 g of Kjeldahl digestion mixture and 5 mL concentrated H_2SO_4 at 250°C for 1 h and 365°C for 2.5–3 h to convert organic nitrogen (N) to ammonium. The digest was diluted to 35 mL, filtered, and analyzed colorimetrically, with results expressed as mg kg^{-1} total N (TN) using the Shimadzu TOC-L combustion method. And total potassium (TK) was determined following a modified UF/IFAS procedure (Mylavarapu, 2002; Soltanpour et al., 1996). Soil samples (0.4 g) were ashed at 500°C–550°C for 5 h, treated with 2 mL of 6 M HCl, reacted for 2 h, diluted with DI water, and analyzed by inductively coupled plasma optical emission spectroscopy.

TC and inorganic carbon (IC) were measured using an Elementar Vario Micro CN analyzer (Elementar Americas Inc.). TC was determined from oven-dried, ground bulk soil, while IC was measured from ash remaining after combustion at 550°C. Organic carbon (OC) was calculated as the difference between TC and IC. Fractionated POM and MAOM samples (4.8–5.2 mg) were weighed into tin capsules and analyzed by combustion using the same CN analyzer to determine POM-C and MAOM-C. TN was measured simultaneously with TC.

Permanganate oxidizable carbon (POXC) was determined using 0.2 M $KMnO_4$ following J. Bhadha et al. (2018) and Chambers et al. (2024). Approximately 2 g of oven-dried soil was reacted with 20 mL of 0.2 M $KMnO_4$ for 2 min, and the filtered supernatant was analyzed at 550 nm using a BioTek Synergy HTX spectrophotometer to quantify oxidizable C. Metal content was analyzed to quantify minerals related to MAOM formation and establish a baseline of mineral content for EAA cultivated histosols for future research. A subsample (0.2–0.3 g) of the ash remaining after LOI was digested with a 1:3 mixture of concentrated HNO_3 and HCl at 96°C for 2 h. After cooling, the digest was filtered through a 0.45-µm polypropylene membrane and analyzed for total metals and

total phosphorus (TP) using inductively coupled plasma mass spectrometry.

2.4.2 | Biological properties

The activities of β-glucosidase, β-glucosaminidase, alkaline phosphatase, and aryl sulfatase were measured using the colorimetric method described by Tabatabai (1994). After sieving through a 2-mm sieve, the soil samples were incubated with modified universal buffer and substrate solutions for each enzyme at 37°C for 1 h. After stopping the reaction with $CaCl_2$ and NaOH, the absorbance of the supernatant was measured at 400 nm. The p-nitrophenol (p-NP) concentration, proportional to enzymatic activity, was quantified using a standard curve.

2.5 | Data analysis

Statistical analyses were conducted using R version 4.5.1 (R Core Team, 2025). For each response variable, linear mixed-effects models (LMMs) were fitted using the *lmer* function from the *lme4* package (Bates et al., 2015). Sampling depth, soil profile thickness, and their interaction were included as fixed effects, while location ID was treated as a random effect to account for spatial dependence among observations. The significance of fixed effects was evaluated using Type III analysis of variance implemented in the *lmerTest* package (Kuznetsova et al., 2017), with degrees of freedom estimated using the Satterthwaite approximation. When significant effects were detected, post hoc pairwise comparisons of estimated marginal means were performed using the *emmeans* package (Lenth, 2024) with Sidak adjustment for multiple comparisons and Kenward–Roger approximation for degrees of freedom. Model assumptions were evaluated by visually inspecting residual plots to assess normality and homogeneity of variance across fitted values. Formal diagnostic tests included the Shapiro–Wilk test for residual normality ($p > 0.05$) and Levene's test for homogeneity of variance ($p > 0.05$). Additional model diagnostics were performed using the *check_model* function from the *performance* package (Lüdecke et al., 2021). When necessary, log transformations were applied to response variables to meet model assumptions. Results are reported as mean ± standard error.

Partial least squares structural equation modeling (PLS-SEM) was used to gain a mechanistic understanding of how soil depth and profile thickness affect MAOM-C and POM-C contents through SHI parameters. PLS-SEM is an approach used to analyze complicated direct and indirect inter-relationships between observed and latent variables. It is robust to small-size data and does not require the assumptions of normal distribution (Hair & Alamer, 2022; Hu et al., 2017). Conceptual models were developed with the hypothesized relationships, assuming soil sample depth and profile thickness influencing the formation of MAOM-C and POM-C through altering the soil properties, including silt, clay, OC, macroaggregates (250 µm–2 mm), microaggregates (<250 µm), activity of β-glucosidase, β-glucosaminidase, alkaline phosphatase, and aryl sulfatase, CEC, pH, calcium (Ca), iron (Fe), and POXC. Models were analyzed for MAOM-C and POM-C separately using the SEMinR package in R (Hair & Alamer, 2022).

3 | RESULTS

3.1 | Soil properties, soil health indicators, and MAOM-C by sampling depth

The EAA soils contained 220.9 ± 9.3 g kg^{-1} TC, which varied significantly with soil sampling depth ($p = 0.003$). OC accounted for 84.0 ± 0.9% ($p = 0.015$), while IC represented 16.0 ± 0.9% of TC ($p = 0.001$) (Figure 2A). By mass, this equated to 184.6 ± 7.2 g OC kg^{-1} and 36.4 ± 2.9 g IC kg^{-1}, from 0 to 45 cm. Both OC and IC decreased with soil sampling depth; OC declined from 198.8 ± 8.3 to 168.5 ± 10.4 g kg^{-1}, while IC decreased from 43.8 ± 4.0 to 25.4 ± 3.6 g kg^{-1} across the depth gradient from 0–15 cm to 30–45 cm. Across all depths, MAOM-C (0.3 ± 0.1 g kg^{-1}) in the EAA soil was substantially lower than POM-C (220.6 ± 9.3 g kg^{-1}). While MAOM-C did not vary significantly with depth ($p = 0.096$), POM-C decreased with sampling depths ($p = 0.003$) (Figure 2B). The ratio of C:N for MAOM-C decreased from 29.2 ± 5.0 to 21.6 ± 1.9 with depth; the C:N for POM-C remained consistent (16.4 ± 0.1) across depths. The C pools MAOM-C, POM-C, OC, and IC did not vary significantly with soil profile thickness or with the interaction between sampling depth and profile thickness ($p > 0.05$). The details are provided in Table 1 and Table S2.

Across sampling depths, ASI did not vary up to 45-cm depth, large macroaggregates (>2 mm), macroaggregates (250 µm–2 mm), microaggregates (53–250 µm), and <53 µm accounted for 49.7 ± 2.6% ($p = 0.537$), 45.7 ± 2.6% ($p = 0.234$), 4.9 ± 0.7% ($p = 0.113$), and 5.6 ± 0.9% ($p = 0.416$), respectively (Figure 3A). Similarly, across all soil depths, POXC remained uniform, averaging 28.2 ± 0.9 g kg^{-1} (Figure 3B). Aggregate size fractions and POXC were also not affected by soil profile thickness or by the interaction between sampling depth and profile thickness ($p > 0.05$), except for microaggregates, which were greater in middle thickness compared to deep profile thickness ($p = 0.027$) (Figure 3A; Table S2).

The EAA soil was mildly alkaline (pH 7.9 ± 0.03) up to 45 cm (Table 1), having no variation by sampling depth ($p = 0.069$). Moisture content increased with depth

TABLE 1 Different soil health indicators (SHIs) of Everglades Agricultural Area (EAA) cultivated histosols by sampling depth.

Type	SHI	Unit	0–15 cm	15–30 cm	30–45 cm	0–45 cm
Physicochemical	Moisture content	%	51.1 ± 1.8[b]	55.3 ± 2.9[ab]	59.6 ± 2.9[b]	55.3 ± 1.6
	Bulk density	g cm^{-3}	0.7 ± 0.04[a]	0.7 ± 0.04[a]	0.7 ± 0.06[a]	0.7 ± 0.03
	Aggregate stability index					
	Large macroaggregates (>2 mm)	%	49.7 ± 4.9[a]	47.8 ± 4.3[a]	52.2 ± 15.4[a]	49.8 ± 2.6
	Macroaggregates (250 µm–2 mm)	%	45.01 ± 4.7[a]	49.0 ± 3.9[a]	42.8 ± 4.8[a]	45.7 ± 2.6
	Microaggregates (53–250 µm)	%	3.6 ± 1.02[a]	4.80 ± 1.3[a]	4.14 ± 1.2[a]	4.9 ± 0.7
	<53 µm fraction	%	7.5 ± 2.7[a]	5.2 ± 3.8[a]	4.1 ± 0.5[a]	5.6 ± 0.9
	POM-C	g kg^{-1}	242.2 ± 11.4[b]	224.04 ± 20.7[ab]	193.7 ± 12.3[a]	220.6 ± 9.3
	MAOM-C		0.4 ± 0.1[a]	0.3 ± 0.1[a]	0.3 ± 0.1[a]	0.3 ± 0.1
	pH	–	8.00 ± 0.06[a]	8.02 ± 0.05[a]	7.9 ± 0.05[a]	7.9 ± 0.03
	CEC	cmolc kg^{-1}	29.01 ± 2.8[a]	29.9 ± 3.03[a]	28.9 ± 2.9[a]	29.3 ± 1.6
	SOM	%	60.8 ± 3.8[a]	61.1 ± 4.2[a]	62.9 ± 3.9[a]	61.6 ± 2.2
	Soil mineral content					
	Clay	%	2.9 ± 0.3[b]	2.3 ± 0.2[ab]	2.1 ± 0.2[a]	2.4 ± 0.1
	Silt		24.8 ± 1.9[a]	24.3 ± 2.6[a]	23.6 ± 2.1[a]	24.2 ± 1.2
	Fine sand		3.6 ± 1.8[a]	3.5 ± 1.2[a]	3.9 ± 1.5[a]	3.7 ± 0.8
	Coarse sand		8.9 ± 1.6[a]	9.6 ± 1.8[a]	7.3 ± 1.4[a]	8.7 ± 0.9
	Soil protein	mg kg^{-1}	473.8 ± 13.8[a]	433.6 ± 25.02[a]	408.9 ± 35.3[a]	439.5 ± 15.1
	POXC	g kg^{-1}	27.9 ± 1.8[a]	27.0 ± 1.5[a]	29.8 ± 1.3[a]	28.2 ± 0.9
	TKN		20.3 ± 2.1[a]	21.1 ± 2.2[a]	21.9 ± 2.1[a]	21.1 ± 1.2
	TK		0.4 ± 0.03[b]	0.3 ± 0.03[ab]	0.3 ± 0.03[a]	0.3 ± 0.02
	TP		18.4 ± 5.5[a]	11.2 ± 2.8[a]	21.6 ± 10.Partial least squares structural equation modeling7[a]	16.9 ± 3.9
	TN		21.2 ± 1.3[a]	20.8 ± 1.7[a]	21.8 ± 1.4[a]	21.3 ± 0.8
	TC		242.6 ± 11.3[b]	224.3 ± 20.7[ab]	193.9 ± 12.3[a]	220.9 ± 9.3
	OC		198.8 ± 8.3[b]	185.2 ± 16.4[ab]	168.5 ± 10.4[a]	184.6 ± 7.2
	IC		43.8 ± 4.01[b]	39.1 ± 5.9[b]	25.4 ± 3.6[a]	36.4 ± 2.9
Biological	**Enzymatic activity**					
	β-Glucosidase	µg p-NP g^{-1} soil h^{-1}	160.9 ± 14.5[b]	116.3 ± 13.1[a]	99.7 ± 11.5[a]	126.6 ± 8.5
	β-Glucosaminidase		291.9 ± 28.5[b]	216.7 ± 24.5[a]	177.6 ± 21.5[a]	229.9 ± 16.01
	Alkaline phosphatase		1137.1 ± 133.6[b]	741.9 ± 84.6[a]	643.4 ± 72.2[a]	845.7 ± 66.4
	Aryl sulfatase		573.3 ± 62.1[b]	389.4 ± 54.8[a]	311.5 ± 40.01[a]	415.2 ± 33.6

Note: Values are presented as mean ± standard error across three depths. Different letters denote the statistical significance ($p < 0.05$) among sampling depths.

Abbreviations: CEC, cation exchange capacity; IC, inorganic carbon; MAOM-C, Carbon within the mineral-associated organic matter; OC, organic carbon; p-NP, p-nitrophenol; POM-C, Carbon within the particulate organic matter; POXC, permanganate oxidizable carbon; SOM, soil organic matter; TC, total carbon; TK, total potassium; TKN, total Kjeldahl nitrogen; TN, total nitrogen; TP, total phosphorus.

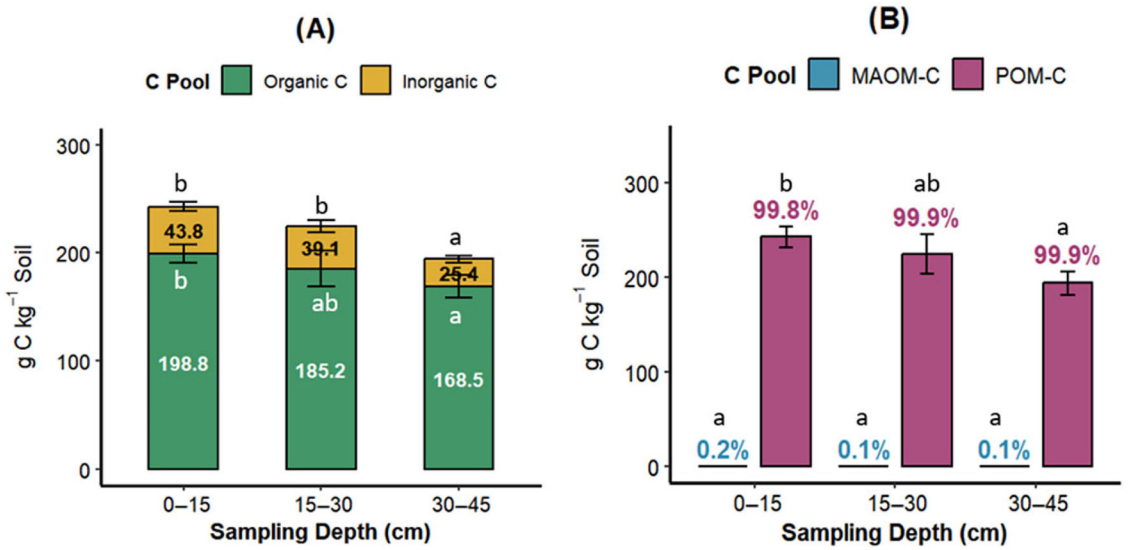

FIGURE 2 Distribution of (A) total C and (B) MAOM-C and POM-C across three sampling depths. Error bars represent the standard error of the mean for each C pool. Different letters indicate significant differences among depths ($p < 0.05$). MAOM-C, Carbon within the mineral-associated organic matter; POM-C, Carbon within the particulate organic matter.

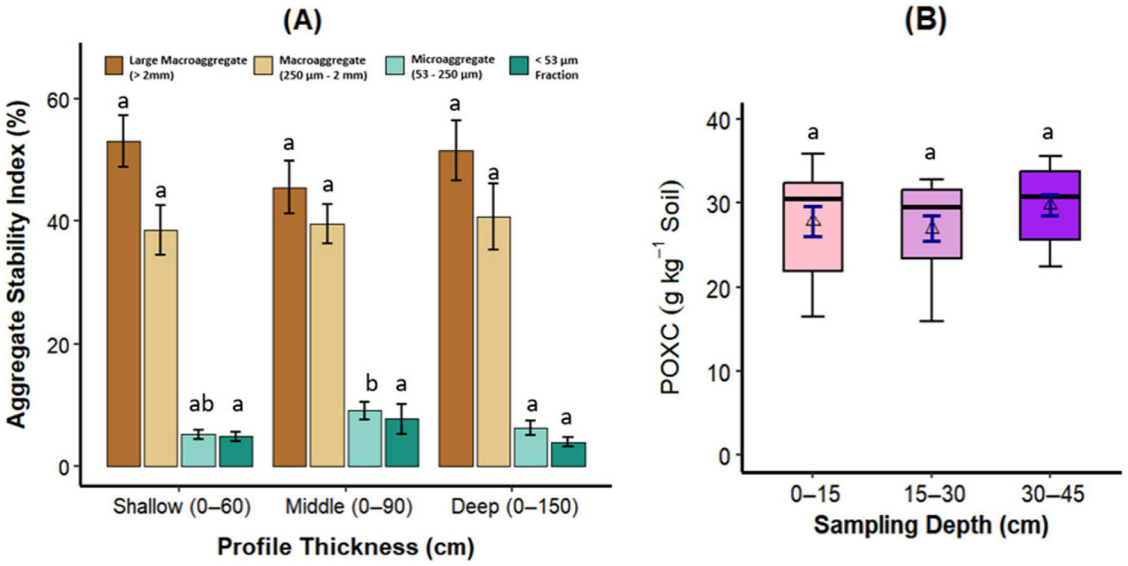

FIGURE 3 Distribution of (A) aggregate stability index (ASI) across profile thickness levels and (B) permanganate oxidizable carbon (POXC) across three sampling depths. Error bars represent the standard error of the mean for each aggregate fraction and POXC. Different letters indicate significant differences among profile thickness levels in (A) and among sampling depths in (B) ($p < 0.05$).

($p = 0.002$), ranging from 51.1 ± 1.8% at 0–15 cm to 59.6 ± 2.9% at 30–45 cm. The tapped bulk density of EAA histosols was 0.70 ± 0.03 g cm^{-3} and did not differ with depth ($p = 0.260$). Similarly, CEC averaged 29.3 ± 1.6 cmolc kg^{-1} throughout ($p = 0.849$). Organic matter averaged 61.6 ± 2.2% by mass and did not vary by depth ($p = 0.826$). Of the inorganic matter, silt had the highest abundance (24.2 ± 1.2% of total soil mass), and clay was the lowest (2.4 ± 0.1%); coarse and fine sand were 8.7 ± 0.9% and 3.7 ± 0.8%, respectively (Figure 4). Among the mineral contents, clay decreased with sampling depth ($p = 0.017$) (Table 1 and Table S2). Of the measured metals, Ca had the highest concentration (54.7 ± 5.6 g kg^{-1}), while cadmium (Cd) had the lowest concentration (0.1 ± 0.01 mg kg^{-1}). The six most abundant metals in the cultivated histosols of the EAA were Ca > magnesium (Mg) > aluminum (Al) > Fe > barium (Ba) > manganese (Mn). These abundant metals did not vary in sampling depth ($p > 0.05$). Other metal concentrations were below 0.3 g kg^{-1} on average. See Table S3 for the analyzed metal content concentrations.

TKN dominated the TN pool, averaging 21.1 ± 1.2 g kg^{-1} with no difference by depth ($p = 0.229$). The average

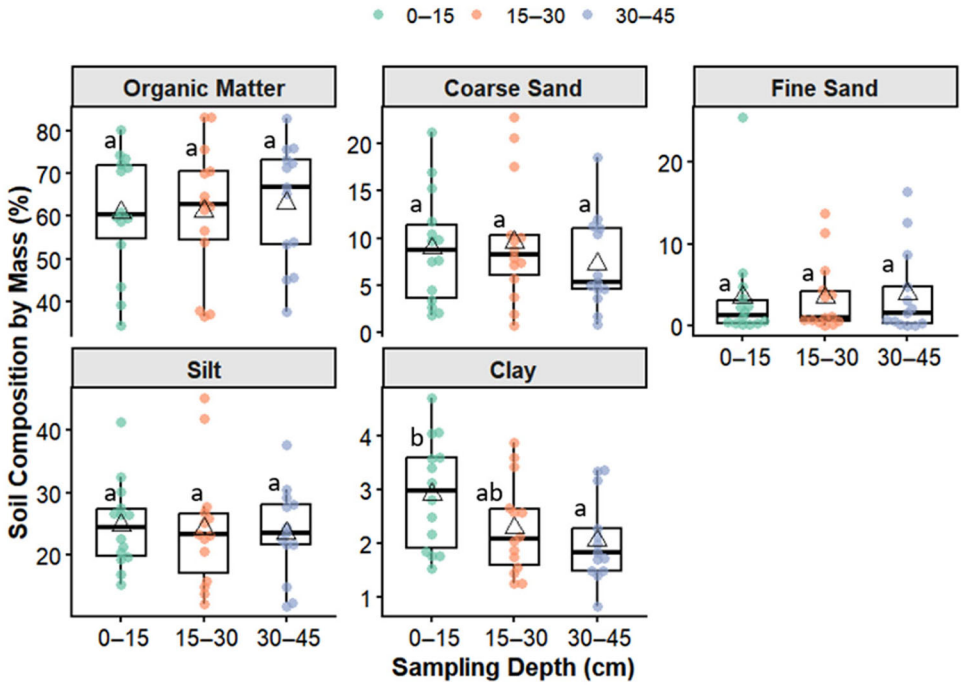

FIGURE 4 Soil composition by mass across three sampling depths. Different letters indicate significant differences among sampling depths for each component ($p < 0.05$).

TN:TP:TK ratio for EAA histosols was 65:38:1 across all depths. The TN of the bulk soil was consistent across depths and averaged 21.3 ± 0.8 g kg^{-1}, resulting in a TC:TN ratio of 10.4 ± 1.0. TK decreased with sampling depth ($p = 0.012$) and showed a sampling depth × profile thickness interaction effect ($p = 0.011$), while profile thickness alone had no effect ($p = 0.623$).

Among the soil enzymes analyzed, alkaline phosphatase exhibited the highest activity (Figure 5), averaging 845.7 ± 66.4 μg p-NP g^{-1} soil h^{-1}, whereas β-glucosidase showed the lowest activity, averaging 126.6 ± 8.5 μg p-NP g^{-1} soil h^{-1}. Unlike most physicochemical properties, enzyme activities declined with depth for β-glucosidase ($p < 0.001$), β-glucosaminidase ($p = 0.002$), alkaline phosphatase ($p < 0.001$), and aryl sulfatase ($p = 0.002$).

3.2 | Predictors of soil carbon stability fractions (MAOM-C and POM-C) across soil properties, SHIs, sampling depth, and profile thickness

The PLS-SEM model explained 36.2% of the variance in MAOM-C (Figure 6). Sampling depth had negative effects on clay content ($p < 0.01$) and on the activity of all four measured enzymes ($p < 0.001$). In contrast, soil profile thickness showed positive effects on β-glucosidase ($p < 0.05$), β-glucosaminidase ($p < 0.01$), alkaline phosphatase ($p < 0.01$), and Fe concentration ($p < 0.01$). However, none of the measured soil properties of SHIs had direct effects on MAOM-C, and no indirect effects of sampling depth or profile thickness on MAOM-C were detected.

The PLS-SEM model explained 86.3% of the variance in POM-C (Figure 7). Similar to the MAOM-C model, sampling depth had negative effects on clay content ($p < 0.01$) and on the activity of all the measured four enzymes ($p < 0.001$). In contrast, soil profile thickness showed positive effects on β-glucosidase ($p < 0.05$), β-glucosaminidase ($p < 0.01$), alkaline phosphatase ($p < 0.01$), and Fe concentration ($p < 0.01$). Unlike MAOM-C, several soil properties did demonstrate direct effects on POM-C, with OC, β-glucosidase activity, and Ca content positively influencing POM-C ($p < 0.05$), indicating that POM-C variability was strongly associated with SOC availability and microbial activity.

4 | DISCUSSION

4.1 | Dominance of POM-C and macroaggregates

Over 99% of soil C in the EAA contained unassociated POM-C, indicating limited physicochemical protection and high vulnerability to mineralization. This dominance of POM-C reflects the inherently low clay content of histosols; clay concentrations were only ~1%–4% across depths (Figure 4), limiting the reactive mineral surfaces required for the formation and stabilization of MAOM. Since organo–mineral

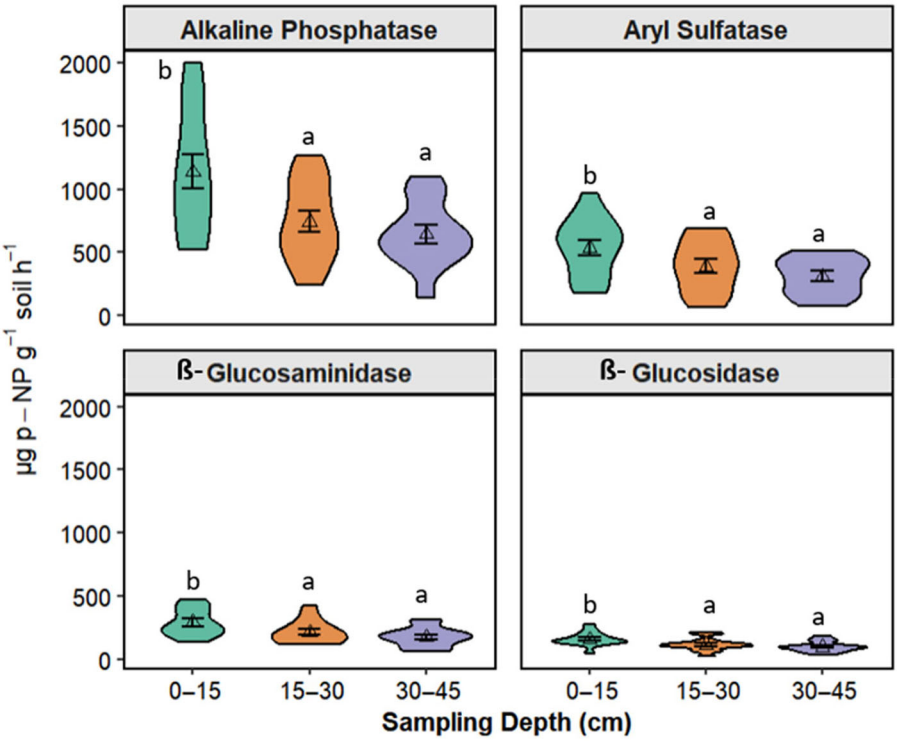

FIGURE 5 Distribution of enzyme activities across three sampling depths. Error bars represent the standard error. Different letters indicate significant differences among sampling depths for each enzyme ($p < 0.05$). p-NP, p-nitrophenol.

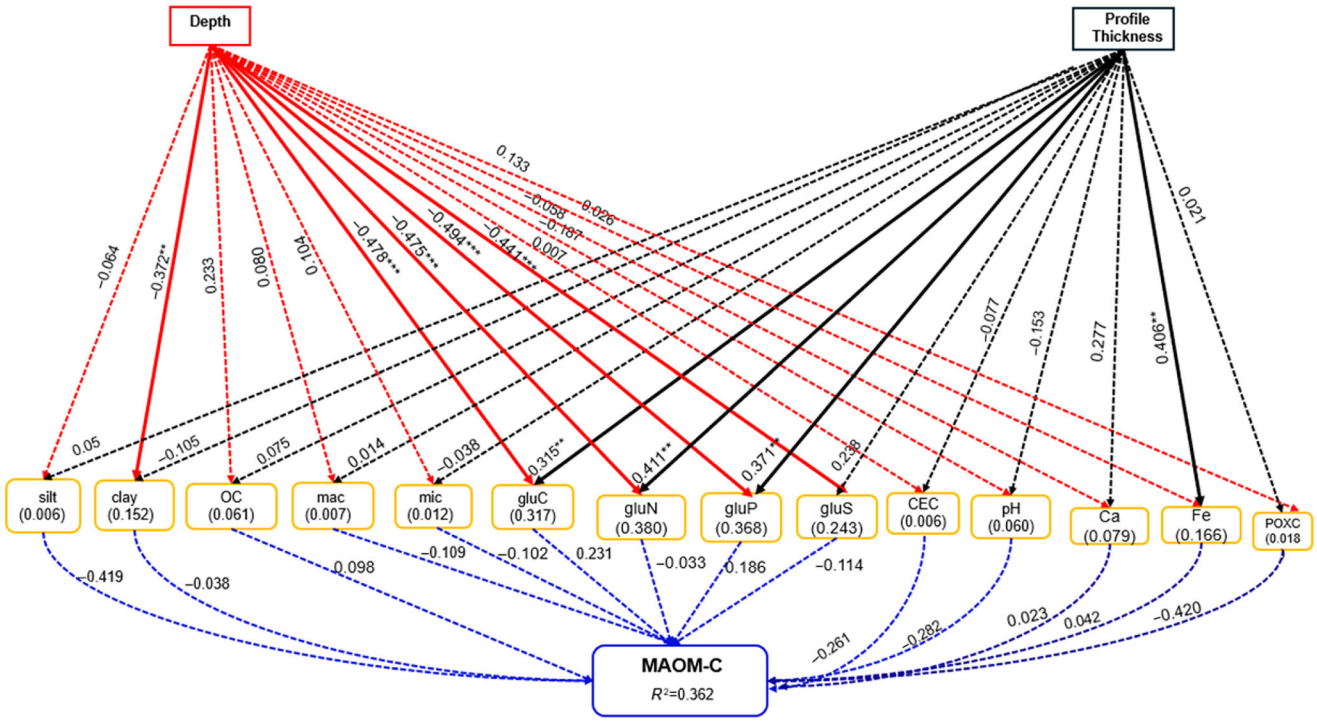

FIGURE 6 Partial least squares structural equation modeling (PLS-SEM) diagram for mineral-associated organic matter-Carbon (MAOM-C). Numbers associated with the arrows are standardized path coefficients with significance (*$p < 0.05$, **$p < 0.01$, ***$p < 0.001$). Dash arrows show nonsignificant relationships ($p > 0.05$). Numbers in parentheses represent the variance explained by the model (R^2). Mac is the content of aggregates with a size larger than 250 μm, including large macroaggregates (> 2mm) and macroaggregates (250 μm2 mm). Mic is aggregates with a size smaller than 250 μm, including microaggregates and <53 μm fraction. gluC, β-glucosidase; gluN, β-glucosaminidase; gluP, alkaline phosphatase; gluS, aryl sulfatas.

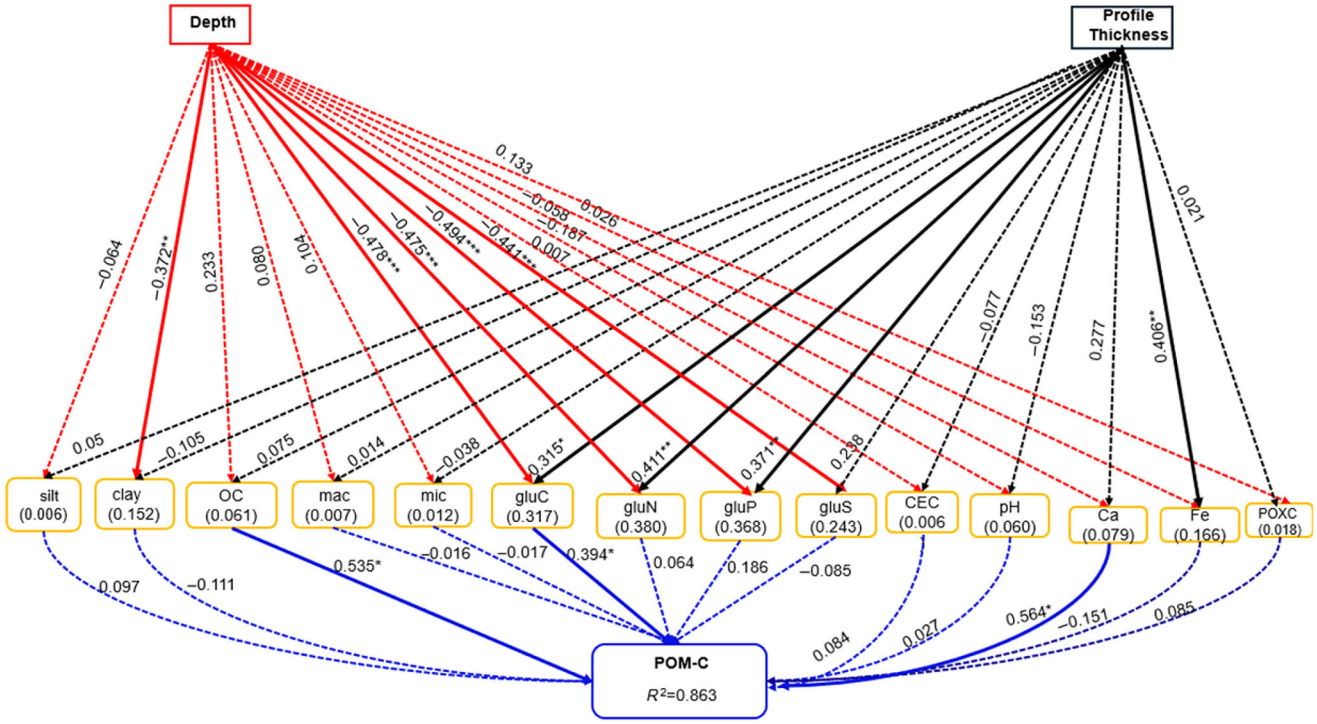

FIGURE 7 Partial least squares structural equation modeling (PLS-SEM) diagram for particulate organic matter-Carbon (POM-C). Numbers associated with the arrows are standardized path coefficients with significance (*$p < 0.05$, **$p < 0.01$, ***$p < 0.001$). Dash arrows show nonsignificant relationships ($p > 0.05$). Numbers in parentheses represent the variance explained by the model (R^2). Mac is the content of aggregates with a size larger than 250 μm, including large macroaggregates (> 2mm) and macroaggregates (250 μm - 2 mm). Mic is aggregates with a size smaller than 250 μm, including microaggregates and <53 μm fraction. gluC, β-glucosidase; gluN, β-glucosaminidase; gluP, alkaline phosphatase; gluS, aryl sulfatas.

associations with clay minerals and metal oxides are key mechanisms of long-term C stabilization, their scarcity may constrain MAOM formation and favor POM accumulation (Cotrufo et al., 2019; Georgiou et al., 2022; Kögel-Knabner et al., 2008; Lehmann & Kleber, 2015). In the EAA, clay content varied little with depth, likely due to subsidence-driven mixing and limited in situ clay formation (Wright et al., 2009). As organic matter oxidizes and soils subside, small amounts of mineral content from underlying limestone and external sources are incorporated into the soil profile, while overall clay concentrations remain very low (J. H. Bhadha et al., 2020; Wright & Hanlon, 2009).

Over 95% of soil ASI was macroaggregates (>250 μm), with microaggregates (53 - 250 μm) comprising less than 5%. Aggregates can protect SOM by entrapping POM and facilitating organo–mineral associations between microbial residues and clay; however, protection generally decreases with increasing aggregate size (Six et al., 2004). While microaggregates are stabilized via coupling organic colloids and clays, macroaggregates are intertwined with plant roots, both live and decomposing, making them sensitive to management practices (Oades, 1984). Thus, microaggregates (<5% of EAA soils) provide greater protection compared to macroaggregates (~95% of EAA soils) due to their ability to encapsulate SOM (Oades, 1984; Tisdall & Oades, 1982). Moreover, in organic-rich histosols, the large aggregates often reflect residual plant fiber cohesion rather than true protective aggregate structures (Totsche et al., 2018), suggesting the stability offered by these complexes may be even less than suggested by high ASI values (Kunarso et al., 2022).

Of note, aggregate stability is strongly influenced by environmental conditions and sample handling, including freezing temperatures (Oztas & Fayetorbay, 2003; Sun et al., 2014), which occurred during sample storage for this study. Prior work demonstrates soil freezing–thawing typically results in a reduction of macroaggregates and a corresponding increase in smaller fractions (Chai et al., 2014; Oztas & Fayetorbay, 2003). To evaluate freezing–thawing effects on ASI in this study, a small-scale comparison of triplicate frozen and nonfrozen samples was conducted (Tables S4A and S4B). The relative standard deviation values for both methods fell within 19% recovery, indicating that freezing did not substantially affect measurements and that if any error was introduced, microaggregate abundance was slightly overestimated.

4.2 | Low abundance of MAOM-C and predictive soil properties for MAOM

Since POM-C dominated EAA soils, MAOM-C was minimal (<1%) and showed little relationship to most measured soil properties or SHIs. Although MAOM formation is generally positively related to silt + clay content (Six et al., 2002), this was not observed in EAA histosols. Despite silt and clay comprising ~26% of the soil mass, MAOM-C remained very low. Similar deviations from a linear relationship between silt + clay content and MAOM-C have been reported in previous studies (Georgiou et al., 2022; Matus, 2021). Furthermore, recent studies indicate that MAOM does not uniformly cover mineral surfaces but accumulates in localized clusters driven by molecular-scale interactions among organic compounds (Schweizer, 2022). In addition, mineral weathering congruency can regulate organo–mineral associations and SOM availability: high congruency enhances decomposition and limits MAOM formation, whereas low congruency promotes mineral protection of organic matter (Fang et al., 2023).

To further examine potential controls on MAOM-C formation beyond particle size, metal concentrations in EAA soils were analyzed. The six most abundant metals: Ca, Mg, Al, Fe, Ba, and Mn were found at average concentrations of at least 1.4 g kg^{-1}. Concentrations of the observed minerals in EAA soils typically remain within the ranges reported in the literature (Kabata-Pendias, 2000; Schwertmann & Tayor, 1989), with the exception of Ca and Mg. The elevated levels of Ca and Mg likely reflect inputs from the weathering of underlying bedrock. Bivalent cations (e.g., Ca^{2+}, Mg^{2+}) can stabilize SOC through cation bridging, while $CaCO_3$ promotes SOC stabilization via aggregation and sorption to mineral matrices (Bronick & Lal, 2005; Rowley et al., 2018, 2021). Mineral crystallinity also influences MAOM formation, with poorly crystalline Fe and Al oxides being more susceptible to degradation than MAOM bound to crystalline minerals (Kleber et al., 2015). Therefore, although metal abundance was quantified, it remains unclear whether the surface properties of the present metals provide favorable conditions for MAOM formation.

Overall, MAOM-C formation in the EAA was not well predicted by fine soil particles, metal content, or common SHIs— only ~36% of the variability in MAOM-C was explained by our data. The low abundance of MAOM may have limited the ability to decipher related properties, or other factors not yet investigated may be important in predicting MAOM abundance. For example, some studies suggest root- and microbe-derived compounds can destabilize MAOM (Li et al., 2021). Oxalic acid, a common root exudate, can release organic compounds from mineral associations and increase microbial access to previously protected compounds (Keiluweit et al., 2015). Likewise, elevated exudation rates facilitate MAOM turnover and limit accumulation (Chari & Taylor, 2022). Therefore, MAOM persistence depends not only on mineral reactivity but also on biochemical soil interactions.

4.3 | Soil depth and profile thickness: Relationship with measured properties

Among measured SHIs, clay content, POM-C, OC, and IC decreased with depth, while moisture content increased. Otherwise, soil properties were largely uniform from 0 to 45 cm, similar to prior studies of SOC variation within the upper soil profile (0–30 cm) (Torres-Sallan et al., 2018). Management practices are known to disproportionately influence near-surface soil properties, with no-till enhancing SOM and aggregation (Kibet et al., 2016) and restoration preferentially increasing POM-C relative to MAOM-C (Wang et al., 2025). Tillage techniques likely contributed to the homogenous characteristics of the soil profile (Zhang et al., 2022). Skadell et al. (2023) reported that, among all agricultural activities with notable SOC effects, 79 ± 7% of the management effects occurred in the topsoil (0–30 cm), 19 ± 3% of effects at 30–50 cm, and 3 ± 4% in the lower subsoil (50–100 cm). Therefore, the 0–45 cm sampling likely captured nearly all management effects and the uniformity of soil C pools, and SHIs was likely attributed to mixing due to agricultural practices.

In contrast, biological activity in the soil was consistently found to be greatest near the top surface and at the root–soil interface. The incorporation of cover crops or organic residues on the soil surface is known to enhance soil enzyme activity (Bandick & Dick, 1999). In rooted soil, microbial biomass increased 17-fold at 10- to 20-cm depth, while β-glucosidase and acid phosphatase activities decreased by 23% and 25%, respectively (Loeppmann et al., 2016). In drained peat systems, however, lowered water tables can stimulate hydrolytic enzyme activity through enhanced aeration and microbial processes (Freeman et al., 1996; Xu et al., 2021), consistent with our observations. To the best of our knowledge, no research has directly quantified the contribution of a specific enzyme to MAOM formation in a cause-and-effect manner. However, numerous studies have explored the overall role of microbial enzymes in facilitating the transformation of organic matter into mineral-associated pools (Cotrufo et al., 2013; Sokol et al., 2019).

Our study was conducted in a region where differential oxidation and subsidence have produced histosols profiles of varying thickness (Rodriguez et al., 2020). A positive relationship between organic matter and profile thickness (Hallema et al., 2015) suggests greater decomposition in

shallower profiles. Hence, profile thickness serves as a proxy for oxidation status, with thicker profiles indicating reduced oxidation and greater resilience, and thinner profiles reflecting advanced degradation. According to the PLS-SEM results (Figures 6 and 7), soil profile thickness positively influenced β-glucosidase, β-glucosaminidase, alkaline phosphatase activities, and Fe concentration, with all variables generally increasing in the deep profile relative to the shallow profile (Table S5). In contrast, the LMMs indicated that microaggregate distribution varied significantly without a consistent directional trend across profile thicknesses; concentrations were similar in the shallow and deep profiles, with the highest abundance in the middle profile. This nonlinear pattern likely reflects a balance between aggregate formation and disruption, with the middle profile providing optimal conditions for aggregation due to the coexistence of organic substrates and mineral components (Six et al., 2004; Tisdall & Oades, 1982).

4.4 | MAOM-C as an indicator of soil stability

Identifying soil properties associated with MAOM-C provides a basis for developing causal links between this indicator of soil stability and existing SHIs. Our results highlight (1) the dominance of POM-C in EAA soils, reflecting a vast, labile (unassociated) pool of soil C, and (2) the lack of other soil properties or existing SHIs that adequately predict the abundance of MAOM-C. A robust body of research supports the concept of C stabilization via MAOM over extended timescales (e.g., Kleber et al., 2021; Marschner et al., 2008; Von Lützow et al., 2007), suggesting that MAOM quantification could be a particularly useful SHI for degraded histosols. The inclusion of MAOM as an SHI in organic-rich soils could offer a more comprehensive and accurate assessment of soil health, particularly in relation to maintaining soil C stocks, improving soil sustainability, and enhancing climate resilience.

5 | CONCLUSIONS

The EAA, a historic peatland, has experienced significant soil subsidence since the early 1900s due to drainage and conversion to agriculture, leading to oxidative loss of histosols. This observational study comprehensively evaluated the conditions of the remaining soil using C fractionation methods and quantifying diverse, well-established SHIs. The distribution of quantified C pools (MAOM-C, POM-C, OC, IC, and POXC), as well as diverse, widely accepted physicochemical SHIs, was observed to be relatively uniform across soil depths up to 45 cm. Only the biological SHIs (i.e., enzyme activities) were significantly impacted by soil depth. The compilation of SHIs suggests that agricultural activities have generally homogenized the top and subsurface soils in the EAA. Unassociated POM-C dominated the soil C pool and varied with depth, indicating a large, labile, and vulnerable C fraction. In contrast, MAOM-C constituted less than 1% of the soil mass and showed no significant relationships with sampling depth, soil profile thickness, soil properties, or SHIs, suggesting minimal physicochemical protection of soil C. These findings highlight a critical gap in understanding the controls on C stabilization in cultivated histosols. Despite its low abundance, MAOM is believed to represent the most stable C fraction and provides unique information not captured by conventional SHIs. Thus, incorporating MAOM as an SHI may improve the assessment of soil stability, particularly in organic soils highly susceptible to oxidation. Future research should evaluate MAOM-C as a potential SHI across diverse soil types (organic, mineral, and transitional) to determine its broader utility for assessing C stability under varying management regimes and pedogenic environments. Furthermore, land management strategies should focus on promoting physicochemical protection of the remaining SOM in the EAA, which could protect soil C stocks, ensure sustainable agriculture, and safeguard the broader Everglades ecosystem.

AUTHOR CONTRIBUTIONS

Mumtahina Riza: Conceptualization; data curation; formal analysis; investigation; methodology; visualization; writing—original draft; writing—review and editing. **Suraj Melkani**: Investigation; methodology; visualization; writing—review and editing. **Noel Manirakiza**: Investigation; methodology; writing—review and editing. **Jehangir H. Bhadha**: Conceptualization; funding acquisition; writing—review and editing. **Zihan Li**: Formal analysis; investigation; writing—review and editing. **Jing Hu**: Conceptualization; formal analysis; funding acquisition; writing—review and editing. **Lisa G. Chambers**: Conceptualization; funding acquisition; investigation; methodology; project administration; resources; supervision; writing—review and editing.

ACKNOWLEDGMENTS

This research was supported by the US Department of Agriculture, National Institute of Food and Agriculture, under Award # 2023-67019-39834 to Lisa G. Chambers, Jehangir H. Bhadha, and Jing Hu. Author Mumtahina Riza was also supported by a Trustees Doctoral Fellowship from the University of Central Florida. The authors would like to thank all Aquatic Biogeochemistry Laboratory members for their lab assistance, especially Sydney Chapman, Tyler Bartczak, and Ava Dennison.

CONFLICT OF INTEREST STATEMENT

The authors declare no conflicts of interest.

ORCID

Mumtahina Riza https://orcid.org/0000-0001-6286-3483
Suraj Melkani https://orcid.org/0009-0000-7489-5335
Jehangir H. Bhadha https://orcid.org/0000-0002-9436-1725
Lisa G. Chambers https://orcid.org/0000-0001-6432-8038

REFERENCES

Aich, S., McVoy, C. W., Dreschel, T. W., & Santamaria, F. (2013). Estimating soil subsidence and carbon loss in the Everglades Agricultural Area, Florida using geospatial techniques. *Agriculture, Ecosystems & Environment*, *171*, 124–133. https://doi.org/10.1016/j.agee.2013.03.017

Andrews, S. S., Karlen, D. L., & Cambardella, C. A. (2004). The Soil Management Assessment Framework: A quantitative soil quality evaluation method. *Soil Science Society of America Journal*, *68*(6), 1945–1962. https://doi.org/10.2136/sssaj2004.1945

Bagnall, D. K., Rieke, E. L., Morgan, C. L. S., Liptzin, D. L., Cappellazzi, S. B., & Honeycutt, C. W. (2023). A minimum suite of soil health indicators for North American agriculture. *Soil Security*, *10*, Article 100084. https://doi.org/10.1016/j.soisec.2023.100084

Bai, X., Zhai, G., Wang, B., An, S., Liu, J., Xue, Z., & Dippold, M. A. (2024). Litter quality controls the contribution of microbial carbon to main microbial groups and soil organic carbon during its decomposition. *Biology and Fertility of Soils*, 167–181. https://doi.org/10.1007/s00374-023-01792-8

Bandick, A. K., & Dick, R. P. (1999). Field management effects on soil enzyme activities. *Soil Biology and Biochemistry*, *31*, 1471–1479.

Bates, D., Mächler, M., Bolker, B., & Walker, S. (2015). Fitting linear mixed-effects models using lme4. *Journal of Statistical Software*, *67*(1), 1–48. https://doi.org/10.18637/jss.v067.i01

Bhadha, J., Khatiwada, R., Galindo, S., Xu, N., & Capasso, J. (2018). Evidence of soil health benefits of flooded rice compared to fallow practice. *Sustainable Agriculture Research*, *7*(4), Article 31. https://doi.org/10.5539/sar.v7n4p31

Bhadha, J. H., Wright, A. L., & Snyder, G. H. (2020). Everglades Agricultural Area soil subsidence and sustainability: SL 311/SS523, rev. 3/2020. *EDIS*, *2020*(2). https://doi.org/10.32473/edis-ss523-2020

Bottcher, A. B., & Izuno, F. T. (1994). *Everglades Agricultural Area (EAA): Water, soil, crop, and environmental management*. University Press of Florida.

Bronick, C. J., & Lal, R. (2005). Soil structure and management: A review. *Geoderma*, *124*(1–2), 3–22. https://doi.org/10.1016/j.geoderma.2004.03.005

Cambardella, C. A., & Elliott, E. T. (1992). Particulate soil organic-matter changes across a grassland cultivation sequence. *Soil Science Society of America Journal*, *56*(3), 777–783. https://doi.org/10.2136/sssaj1992.03615995005600030017x

Cambardella, C. A., & Elliott, E. T. (1993). Carbon and nitrogen distribution in aggregates from cultivated and native grassland soils. *Soil Science Society of America Journal*, *57*(4), 1071–1076. https://doi.org/10.2136/sssaj1993.03615995005700040032x

Chai, Y. J., Zeng, X. B., E, S. Z., Bai, L. Y., Su, S. M., & Huang, T. (2014). Effects of freeze–thaw on aggregate stability and the organic carbon and nitrogen enrichment ratios in aggregate fractions. *Soil Use and Management*, *30*(4), 507–516. https://doi.org/10.1111/sum.12153

Chambers, L. G., Mirabito, A. J., Brew, S., Nitsch, C. K., Bhadha, J. H., Hurst, N. R., & Berkowitz, J. F. (2024). Evaluating permanganate oxidizable carbon (POXC)'s potential for differentiating carbon pools in wetland soils. *Ecological Indicators*, *167*, Article 112624. https://doi.org/10.1016/j.ecolind.2024.112624

Chapman, H. D. (1965). Cation-exchange capacity. In A. G. Norman (Ed.), *Methods of soil analysis. Part 2: Chemical and microbiological properties* (pp. 891–901). ASA, CSSA, SSSA. https://acsess.onlinelibrary.wiley.com/doi/pdf/10.2134/agronmonogr9.2

Chari, N. R., & Taylor, B. N. (2022). Soil organic matter formation and loss are mediated by root exudates in a temperate forest. *Nature Geoscience*, *15*(12), 1011–1016. https://doi.org/10.1038/s41561-022-01079-x

Conchedda, G., & Tubiello, F. N. (2020). Drainage of organic soils and GHG emissions: Validation with country data. *Earth System Science Data*, *12*(4), 3113–3137. https://doi.org/10.5194/essd-12-3113-2020

Cotrufo, M. F., Ranalli, M. G., Haddix, M. L., Six, J., & Lugato, E. (2019). Soil carbon storage informed by particulate and mineral-associated organic matter. *Nature Geoscience*, *12*(12), 989–994. https://doi.org/10.1038/s41561-019-0484-6

Cotrufo, M. F., Wallenstein, M. D., Boot, C. M., Denef, K., & Paul, E. A. (2013). The Microbial Efficiency-Matrix Stabilization (MEMS) framework integrates plant litter decomposition with soil organic matter stabilization: Do labile plant inputs form stable soil organic matter? *Global Change Biology*, *19*, 988–995. https://doi.org/10.1111/gcb.12113

Fang, Q., Lu, A., Hong, H., Kuzyakov, Y., Algeo, T. J., Zhao, L., Olshansky, Y., Moravec, B., Barrientes, D. M., & Chorover, J. (2023). Mineral weathering is linked to microbial priming in the critical zone. *Nature Communications*, *14*(1), Article 345. https://doi.org/10.1038/s41467-022-35671-x

Feng, W., Plante, A. F., & Six, J. (2013). Improving estimates of maximal organic carbon stabilization by fine soil particles. *Biogeochemistry*, *112*(1–3), 81–93. https://doi.org/10.1007/s10533-011-9679-7

Freeman, C., Liska, G., Ostle, N. J., Lock, M. A., Reynolds, B., & Hudson, J. (1996). Microbial activity and enzymic decomposition processes following peatland water table drawdown. *Plant and Soil*, *180*(1), 121–127. https://doi.org/10.1007/BF00015418

Georgiou, K., Jackson, R. B., Vindušková, O., Abramoff, R. Z., Ahlström, A., Feng, W., Harden, J. W., Pellegrini, A. F. A., Polley, H. W., Soong, J. L., Riley, W. J., & Torn, M. S. (2022). Global stocks and capacity of mineral-associated soil organic carbon. *Nature Communications*, *13*(1), Article 3797. https://doi.org/10.1038/s41467-022-31540-9

Ghani, A., Dexter, M., & Perrott, K. W. (2003). Hot-water extractable carbon in soils: A sensitive measurement for determining impacts of fertilisation, grazing and cultivation. *Soil Biology and Biochemistry*, *35*(9), 1231–1243. https://doi.org/10.1016/S0038-0717(03)00186-X

Hair, J., & Alamer, A. (2022). Partial least squares structural equation modeling (PLS-SEM) in second language and education research: Guidelines using an applied example. *Research Methods in Applied Linguistics*, *1*(3), Article 100027. https://doi.org/10.1016/j.rmal.2022.100027

Hallema, D. W., Lafond, J. A., Périard, Y., Gumiere, S. J., Sun, G., & Caron, J. (2015). Long-term effects of peatland cultivation on soil physical and hydraulic properties: Case study in Canada. *Vadose Zone Journal*, *14*(6), 1–12. https://doi.org/10.2136/vzj2014.10.0147

Hu, J., VanZomeren, C. M., Inglett, K. S., Wright, A. L., Clark, M. W., & Reddy, K. R. (2017). Greenhouse gas emissions under differ-

ent drainage and flooding regimes of cultivated peatlands. *Journal of Geophysical Research: Biogeosciences*, *122*(11), 3047–3062. https://doi.org/10.1002/2017JG004010

Izuno, F. T., Sanchez, C. A., Coale, F. J., Bottcher, A. B., & Jones, D. B. (1991). Phosphorus concentrations in drainage water in the Everglades Agricultural Area. *Journal of Environmental Quality*, *20*(3), 608–619. https://doi.org/10.2134/jeq1991.00472425002000030018x

Jacobs, H. S., Reed, R. M., Thien, S. J., & Withee, L. V. (Eds.). (1964). *Soils laboratory exercise source book*. American Society of Agronomy.

Jagadamma, S., Mayes, M. A., Steinweg, J. M., & Schaeffer, S. M. (2014). Substrate quality alters the microbial mineralization of added substrate and soil organic carbon. *Biogeosciences*, *11*(17), 4665–4678. https://doi.org/10.5194/bg-11-4665-2014

Kabata-Pendias, A. (2000). *Trace elements in soils and plants* (3rd ed.). CRC Press.

Kaiser, M., Kleber, M., & Berhe, A. A. (2015). How air-drying and rewetting modify soil organic matter characteristics: An assessment to improve data interpretation and inference. *Soil Biology and Biochemistry*, *80*, 324–340. https://doi.org/10.1016/j.soilbio.2014.10.018

Karami, A., Homaee, M., Afzalinia, S., Ruhipour, H., & Basirat, S. (2012). Organic resource management: Impacts on soil aggregate stability and other soil physico-chemical properties. *Agriculture, Ecosystems & Environment*, *148*, 22–28. https://doi.org/10.1016/j.agee.2011.10.021

Keiluweit, M., Bougoure, J. J., Nico, P. S., Pett-Ridge, J., Weber, P. K., & Kleber, M. (2015). Mineral protection of soil carbon counteracted by root exudates. *Nature Climate Change*, *5*(6), 588–595. https://doi.org/10.1038/nclimate2580

Kemper, W. D., & Rosenau, R. C. (1986). Aggregate stability and size distribution. In A. Klute (Ed.), *Methods of soil analysis. Part 1: Physical and mineralogical methods* (pp. 425–442). Soil Science Society of America, American Society of Agronomy. https://doi.org/10.2136/sssabookser5.1.2ed.c17

Kibet, L. C., Blanco-Canqui, H., & Jasa, P. (2016). Long-term tillage impacts on soil organic matter components and related properties on a Typic Argiudoll. *Soil and Tillage Research*, *155*, 78–84. https://doi.org/10.1016/j.still.2015.05.006

Kleber, M., Bourg, I. C., Coward, E. K., Hansel, C. M., Myneni, S. C. B., & Nunan, N. (2021). Dynamic interactions at the mineral–organic matter interface. *Nature Reviews Earth & Environment*, *2*(6), 402–421. https://doi.org/10.1038/s43017-021-00162-y

Kleber, M., Eusterhues, K., Keiluweit, M., Mikutta, C., Mikutta, R., & Nico, P. S. (2015). Mineral–organic associations: Formation, properties, and relevance in soil environments. In D. L. Sparks (Ed.), *Advances in agronomy* (Vol. 130, pp. 1–140). Academic Press. https://doi.org/10.1016/bs.agron.2014.10.005

Kögel-Knabner, I., Guggenberger, G., Kleber, M., Kandeler, E., Kalbitz, K., Scheu, S., Eusterhues, K., & Leinweber, P. (2008). Organo-mineral associations in temperate soils: Integrating biology, mineralogy, and organic matter chemistry. *Journal of Plant Nutrition and Soil Science*, *171*, 61–82. https://doi.org/10.1002/jpln.200700048

Kunarso, A., Bonner, M. T. L., Blanch, E. W., & Grover, S. (2022). Differences in tropical peat soil physical and chemical properties under different land uses: A systematic review and meta-analysis. *Journal of Soil Science and Plant Nutrition*, *22*(4), 4063–4083. https://doi.org/10.1007/s42729-022-01008-2

Kuznetsova, A., Brockhoff, P. B., & Christensen, R. H. B. (2017). lmerTest package: Tests in linear mixed effects models. *Journal of Statistical Software*, *82*(13), 1–26. https://doi.org/10.18637/jss.v082.i13

Lavallee, J. M., Soong, J. L., & Cotrufo, M. F. (2020). Conceptualizing soil organic matter into particulate and mineral-associated forms to address global change in the 21st century. *Global Change Biology*, *26*(1), 261–273. https://doi.org/10.1111/gcb.14859

Lehmann, J., & Kleber, M. (2015). The contentious nature of soil organic matter. *Nature*, *528*(7580), 60–68. https://doi.org/10.1038/nature16069

Lenth, R. V. (2024). emmeans: Estimated Marginal Means, aka Least-Squares Means (R package version 1.10.2) [Computer software]. CRAN. https://CRAN.R-project.org/package=emmeans

Lessmann, M., Ros, G. H., Young, M. D., & De Vries, W. (2022). Global variation in soil carbon sequestration potential through improved cropland management. *Global Change Biology*, *28*(3), 1162–1177. https://doi.org/10.1111/gcb.15954

Li, H., Bölscher, T., Winnick, M., Tfaily, M. M., Cardon, Z. G., & Keiluweit, M. (2021). Simple plant and microbial exudates destabilize mineral-associated organic matter via multiple pathways. *Environmental Science & Technology*, *55*(5), 3389–3398. https://doi.org/10.1021/acs.est.0c04592

Loeppmann, S., Semenov, M., Blagodatskaya, E., & Kuzyakov, Y. (2016). Substrate quality affects microbial and enzyme activities in rooted soil. *Journal of Plant Nutrition and Soil Science*, *179*, 39–47. https://doi.org/10.1002/jpln.201400518

Lüdecke, D., Ben-Shachar, M. S., Patil, I., Waggoner, P., & Makowski, D. (2021). performance: An R package for assessment, comparison and testing of statistical models. *Journal of Open Source Software*, *6*(60), Article 3139. https://doi.org/10.21105/joss.03139

Marschner, B., Brodowski, S., Dreves, A., Gleixner, G., Gude, A., Grootes, P. M., Hamer, U., Heim, A., Jandl, G., Ji, R., Kaiser, K., Kalbitz, K., Kramer, C., Leinweber, P., Rethemeyer, J., Schäffer, A., Schmidt, M. W. I., Schwark, L., & Wiesenberg, G. L. B. (2008). How relevant is recalcitrance for the stabilization of organic matter in soils? *Journal of Plant Nutrition and Soil Science*, *171*(1), 91–110. https://doi.org/10.1002/jpln.200700049

Matus, F. J. (2021). Fine silt and clay content is the main factor defining maximal C and N accumulations in soils: A meta-analysis. *Scientific Reports*, *11*(1), Article 6438. https://doi.org/10.1038/s41598-021-84821-6

Mirabito, A. J., & Chambers, L. G. (2023). Quantifying mineral-associated organic matter in wetlands as an indicator of the degree of soil carbon protection. *Geoderma*, *430*, Article 116327. https://doi.org/10.1016/j.geoderma.2023.116327

Moebius-Clune, B. N. (2016). *Comprehensive assessment of soil health: The Cornell framework manual* (3rd ed.). Cornell University.

Mylavarapu, R. S. (2002). *UF/IFAS extension soil testing laboratory (ESTL) analytical procedures and training manual*. University of Florida. https://ufdcimages.uflib.ufl.edu/IR/00/00/34/69/00001/SS31200.pdf

Nelson, D. W., & Sommers, L. E. (1996). Total carbon, organic carbon, and organic matter. In D. L. Sparks, A. L. Page, P. A. Helmke, R. H. Loeppert, P. N. Soltanpour, M. A. Tabatabai, C. T. Johnston, & M. E. Sumner (Eds.), *Methods of soil analysis. Part 3: Chemical methods* (pp. 961–1010). Soil Science Society of America, American Society of Agronomy. https://doi.org/10.2136/sssabookser5.3.c34

Oades, J. M. (1984). Soil organic matter and structural stability: Mechanisms and implications for management. *Plant and Soil*, *76*, 319–337.

Osborne, T. Z., Fitz, H. C., & Davis, S. E. (2017). Restoring the foundation of the Everglades ecosystem: Assessment of edaphic responses to hydrologic restoration scenarios. *Restoration Ecology*, *25*(S1), S59–S70. https://doi.org/10.1111/rec.12496

Oztas, T., & Fayetorbay, F. (2003). Effect of freezing and thawing processes on soil aggregate stability. *Catena*, *52*(1), 1–8. https://doi.org/10.1016/S0341-8162(02)00177-7

R Core Team. (2025). *R: A Language and Environment for Statistical Computing (Version 4.5.1) [Computer software]*. R Foundation for Statistical Computing. https://www.R-project.org/

Rice, R. W., Gilbert, R. A., & Daroub, S. H. (2005). *Application of the soil taxonomy key to the organic soils of the Everglades Agricultural Area*. University of Florida.

Rodriguez, A. F., Gerber, S., & Daroub, S. H. (2020). Modeling soil subsidence in a subtropical drained peatland. The case of the Everglades Agricultural Area. *Ecological Modelling*, *415*, Article 108859. https://doi.org/10.1016/j.ecolmodel.2019.108859

Rowley, M. C., Grand, S., Spangenberg, J. E., & Verrecchia, E. P. (2021). Evidence linking calcium to increased organo-mineral association in soils. *Biogeochemistry*, *153*(3), 223–241. https://doi.org/10.1007/s10533-021-00779-7

Rowley, M. C., Grand, S., & Verrecchia, É. P. (2018). Calcium-mediated stabilisation of soil organic carbon. *Biogeochemistry*, *137*(1–2), 27–49. https://doi.org/10.1007/s10533-017-0410-1

Schindelbeck, R., Moebius-Clune, B., Moebius-Clune, D., Kurtz, K., & van Es, H. (2016). *Cornell soil health laboratory: Comprehensive assessment of soil health standard operating procedures*. Cornell University.

Schweizer, S. A. (2022). Perspectives from the Fritz-Scheffer Awardee 2021: Soil organic matter storage and functions determined by patchy and piled-up arrangements at the microscale. *Journal of Plant Nutrition and Soil Science*, *185*, 694–706. https://doi.org/10.1002/jpln.202200217

Schwertmann, U., & Tayor, R. M. (1989). Iron oxides. In J. B. Dixon & S. B. Weed (Eds.), *Minerals in soil environment* (2nd ed., pp. 379–438). ASA, CSSA, SSSA.

Six, J., Bossuyt, H., Degryze, S., & Denef, K. (2004). A history of research on the link between (micro)aggregates, soil biota, and soil organic matter dynamics. *Soil and Tillage Research*, *79*(1), 7–31. https://doi.org/10.1016/j.still.2004.03.008

Six, J., Conant, R. T., Paul, E. A., & Paustian, K. (2002). Stabilization mechanisms of soil organic matter: Implications for C-saturation of soils. *Plant and Soil*, *241*, 155–176.

Six, J., Elliott, E. T., Paustian, K., & Doran, J. W. (1998). Aggregation and soil organic matter accumulation in cultivated and native grassland soils. *Soil Science Society of America Journal*, *62*(5), 1367–1377. https://doi.org/10.2136/sssaj1998.03615995006200050032x

Skadell, L. E., Schneider, F., Gocke, M. I., Guigue, J., Amelung, W., Bauke, S. L., Hobley, E. U., Barkusky, D., Honermeier, B., Kögel-Knabner, I., Schmidhalter, U., Schweitzer, K., Seidel, S. J., Siebert, S., Sommer, M., Vaziritabar, Y., & Don, A. (2023). Twenty percent of agricultural management effects on organic carbon stocks occur in subsoils—Results of ten long-term experiments. *Agriculture, Ecosystems & Environment*, *356*, Article 108619. https://doi.org/10.1016/j.agee.2023.108619

Soil Survey Staff. (2022). *Keys to soil taxonomy* (13th ed.). U.S. Department of Agriculture, Natural Resources Conservation Service.

Sokol, N. W., Kuebbing, S. E., Karlsen-Ayala, E., & Bradford, M. A. (2019). Evidence for the primacy of living root inputs, not root or shoot litter, in forming soil organic carbon. *New Phytologist*, *221*(1), 233–246. https://doi.org/10.1111/nph.15361

Soltanpour, P. N., Johnson, G. W., Workman, S. M., Jones, J. B., & Miller, R. O. (1996). Inductively Coupled Plasma Emission Spectrometry and Inductively Coupled Plasma-Mass Spectrometry. In D. L. Sparks, A. L. Page, P. A. Helmke, R. H. Loeppert, P. N. Soltanpour, M. A. Tabatabai, C. T. Johnston, & M. E. Sumner (Eds.), *Methods of soil analysis. Part 3: Chemical methods* (pp. 91–139). Soil Science Society of America, American Society of Agronomy. https://doi.org/10.2136/sssabookser5.3.c5

Sun, T., Chen, Q., Chen, Y., Cruse, R. M., Li, X. F., Song, C. Y., Kravchenko, Y. S., & Zhang, X. Y. (2014). A novel soil wetting technique for measuring wet stable aggregates. *Soil and Tillage Research*, *141*, 19–24. https://doi.org/10.1016/j.still.2014.03.009

Tabatabai, M. (1994). Soil enzymes. *Methods of Soil Analysis: Part 2 Microbiological and Biochemical Properties*, *5*, 775–833.

Tiemeyer, B., Freibauer, A., Borraz, E. A., Augustin, J., Bechtold, M., Beetz, S., Beyer, C., Ebli, M., Eickenscheidt, T., Fiedler, S., Förster, C., Gensior, A., Giebels, M., Glatzel, S., Heinichen, J., Hoffmann, M., Höper, H., Jurasinski, G., Laggner, A., … Drösler, M. (2020). A new methodology for organic soils in national greenhouse gas inventories: Data synthesis, derivation and application. *Ecological Indicators*, *109*, Article 105838. https://doi.org/10.1016/j.ecolind.2019.105838

Tisdall, J. M., & Oades, J. M. (1982). Organic matter and water-stable aggregates in soils. *Journal of Soil Science*, *33*(2), 141–163. https://doi.org/10.1111/j.1365-2389.1982.tb01755.x

Torres-Sallan, G., Creamer, R. E., Lanigan, G. J., Reidy, B., & Byrne, K. A. (2018). Effects of soil type and depth on carbon distribution within soil macroaggregates from temperate grassland systems. *Geoderma*, *313*, 52–56. https://doi.org/10.1016/j.geoderma.2017.10.012

Totsche, K. U., Amelung, W., Gerzabek, M. H., Guggenberger, G., Klumpp, E., Knief, C., Lehndorff, E., Mikutta, R., Peth, S., Prechtel, A., Ray, N., & Kögel-Knabner, I. (2018). Microaggregates in soils. *Journal of Plant Nutrition and Soil Science*, *181*(1), 104–136. https://doi.org/10.1002/jpln.201600451

Von Lützow, M., Kögel-Knabner, I., Ekschmitt, K., Flessa, H., Guggenberger, G., Matzner, E., & Marschner, B. (2007). SOM fractionation methods: Relevance to functional pools and to stabilization mechanisms. *Soil Biology and Biochemistry*, *39*(9), 2183–2207. https://doi.org/10.1016/j.soilbio.2007.03.007

Wang, X., Song, Z., Yang, X., Kuzyakov, Y., Fang, Y., Guo, L., Hartley, I. P., Li, Q., Wu, L., Zhang, Z., Ran, X., Wang, W., Wang, Y., Li, Y., Luo, Y., Xia, S., Wang, Z., Luo, Z., Chen, J., … Wang, H. (2025). Distribution, storage, and factors influencing particulate and mineral-associated organic matter in paddy soils. *Global Biogeochemical Cycles*, *39*(9), Article e2025GB008577. https://doi.org/10.1029/2025GB008577

Wienhold, B. J., Karlen, D. L., Andrews, S. S., & Stott, D. E. (2009). Protocol for Soil Management Assessment Framework (SMAF) soil indicator scoring curve development. *Renewable Agriculture and Food Systems*, *24*(6), 260–266.

Wright, A. L., & Hanlon, E. A. (2009). Soil structure in Everglades Agricultural Area histosols: Effects on carbon sequestration and subsidence: SL 301/SS514, 8/2009. *EDIS*, *2009*(7). https://doi.org/10.32473/edis-ss514-2009

Wright, A. L., & Inglett, P. W. (2009). Soil organic carbon and nitrogen and distribution of carbon-13 and nitrogen-15 in aggregates of Everglades histosols. *Soil Science Society of America Journal*, *73*(2), 427–433..

Wright, A. L., Ramesh Reddy, K., & Newman, S. (2009). Microbial indicators of eutrophication in Everglades wetlands. *Soil Science Society of America Journal*, *73*(5), 1597–1603. https://doi.org/10.2136/sssaj2009.0083

Xu, Z., Wang, S., Wang, Z., Dong, Y., Zhang, Y., Liu, S., & Li, J. (2021). Effect of drainage on microbial enzyme activities and communities dependent on depth in peatland soil. *Biogeochemistry*, *155*(3), 323–341. https://doi.org/10.1007/s10533-021-00828-1

Zhang, Q., Zhang, Y., Wang, X., Li, H., Liu, P., Wang, X., Wang, R., & Li, J. (2022). Change of tillage system affects the soil carbon pools characters, reduces carbon emissions and improves maize yield in the Loess Plateau. *European Journal of Agronomy*, *141*, Article 126614. https://doi.org/10.1016/j.eja.2022.126614

SUPPORTING INFORMATION

Additional supporting information can be found online in the Supporting Information section at the end of this article.

How to cite this article: Riza, M., Melkani, S., Manirakiza, N., Bhadha, J. H., Li, Z., Hu, J., & Chambers, L. G. (2026). Mineral-associated organic matter and soil health indicators in subsiding cultivated histosols of the Everglades Agricultural Area. *Soil Science Society of America Journal*, *90*, e70254. https://doi.org/10.1002/saj2.70254